Separation Science and Technology
Publication details, including instructions for authors and subscription information:
http://www.informaworld.com/smpp/title~content=t713708471

Design of a Simulated Moving Bed: Optimal Particle Size of the Stationary Phase

Olivier Ludemann-Hombourger[a]; Michel Bailly[b]; Roger Marc Nicoud[a]
[a] NOVASEP, VANDOEUVERE-LÈS-NANCY, FRANCE [b] LABORATOIRE DES SCIENCES DU GÉNIE CHIMIQUE, NANCY CEDEX, FRANCE

Online publication date: 13 June 2000

To cite this Article Ludemann-Hombourger, Olivier , Bailly, Michel and Nicoud, Roger Marc(2000) 'Design of a Simulated Moving Bed: Optimal Particle Size of the Stationary Phase', Separation Science and Technology, 35: 9, 1285 — 1305
To link to this Article: DOI: 10.1081/SS-100100225
URL: http://dx.doi.org/10.1081/SS-100100225

SEPARATION SCIENCE AND TECHNOLOGY, **35**(9), pp. 1285–1305, 2000

Design of a Simulated Moving Bed: Optimal Particle Size of the Stationary Phase

OLIVIER LUDEMANN-HOMBOURGER
NOVASEP
15, RUE DU BOIS DE LA CHAMPELLE, PARC TECHNOLOGIQUE DE BRABOIS
BP 50, 5450 VANDOEUVERE-LÈS-NANCY, FRANCE

MICHEL BAILLY
LABORATOIRE DES SCIENCES DU GÉNIE CHIMIQUE
1 RUE GRANDVILLE, BP 451, 54001 NANCY CEDEX, FRANCE

ROGER MARC NICOUD*
NOVASEP
15, RUE DU BOIS DE LA CHAMPELLE, PARC TECHNOLOGIQUE DE BRABOIS
BP 50, 5450 VANDOEUVERE-LÈS-NANCY, FRANCE

ABSTRACT

The influence of the particle size on simulated moving bed (SMB) design is studied using the chiral separation of methyl mandelate on Chiralcel OD. The theoretical model of the pressure drop and band dispersion is validated with experimental results obtained with two different particle sizes (20 and 50 μm) using linear adsorption isotherms. The influence of the particle size on the SMB column size and productivity shows that the optimum particle size is 20–25 μm when working with an acceptable column length and a minimum amount of stationary phase. Due to the high cost of the coated silica stationary phases used for chiral separation, the separation cost is thus minimized.

INTRODUCTION

The simulated moving bed (SMB) was developed in the late 1950s for the purification of *p*-xylene on a very large scale (1). More than 100 production plants have been implemented around the world in the petrochemical and food

* To whom correspondence should be addressed.

processing industries (2), leading to production capacities of up to 100,000 tons per year.

The development in the 1980s of laboratory-scale systems (3) combined with the simultaneous development of new, efficient chiral stationary phases (4, 5) has led to rapid acceptance of the technique in the pharmaceutical industry. As a result of the increasing demands in this area SMB is now considered an attractive tool for the separation of chiral compounds (6).

The main advantages of this technique correspond to the two main requirements of drug development:

- Short development time (SMB uses robust simulation software).
- Low cost and risk. Competitive process like crystallization and enantioselective synthesis are, in most cases, more expensive.

The best and simplest solution is to combine an SMB separation with a simple racemic synthesis and possibly to racemize the collected unwanted enantiomer to increase yields. Production-scale plants are now implemented for performing multiton-scale separation of optical isomers. In order to get the best separation performances from the system, it is necessary to optimize each parameter of the system. The optimization of the particle size of the stationary phase is discussed here to show its major influence on the cost of the separation.

BASIC PRINCIPLES

The relatively low productivity of classical elution chromatography and the discontinuity of the process can be overcome with a countercurrent process where the flow of the solid phase is countercurrent to that of the liquid in the column. This true moving bed configuration (TMB) is shown in Fig. 1. The feed mixture of a binary (or pseudobinary) mixture is continuously injected at one point in this column. The velocity of both the solid and liquid phases can be selected so that the more retained compound moves in the direction of the solid phase whereas the less retained compound is eluted by the liquid phase. The two fractions can then be collected at the extract and raffinate points of this system. The injection of eluent is necessary to avoid the recirculation of the products throughout the system.

The calculation of the TMB optimal flow rates has been largely described for linear (3, 7) and nonlinear (8, 9) adsorption isotherms.

Circulation of the solid phase is difficult to achieve due to displacement of the particles. To overcome this problem it is necessary to modify the initial concept of a moving solid phase with fixed inlet and outlet points. In the modification the solid phase is fixed but the inlet and outlet points are moved. The simulated moving bed configuration is illustrated in Fig. 2: columns are con-

MARCEL DEKKER, INC.
270 Madison Avenue, New York, New York 10016

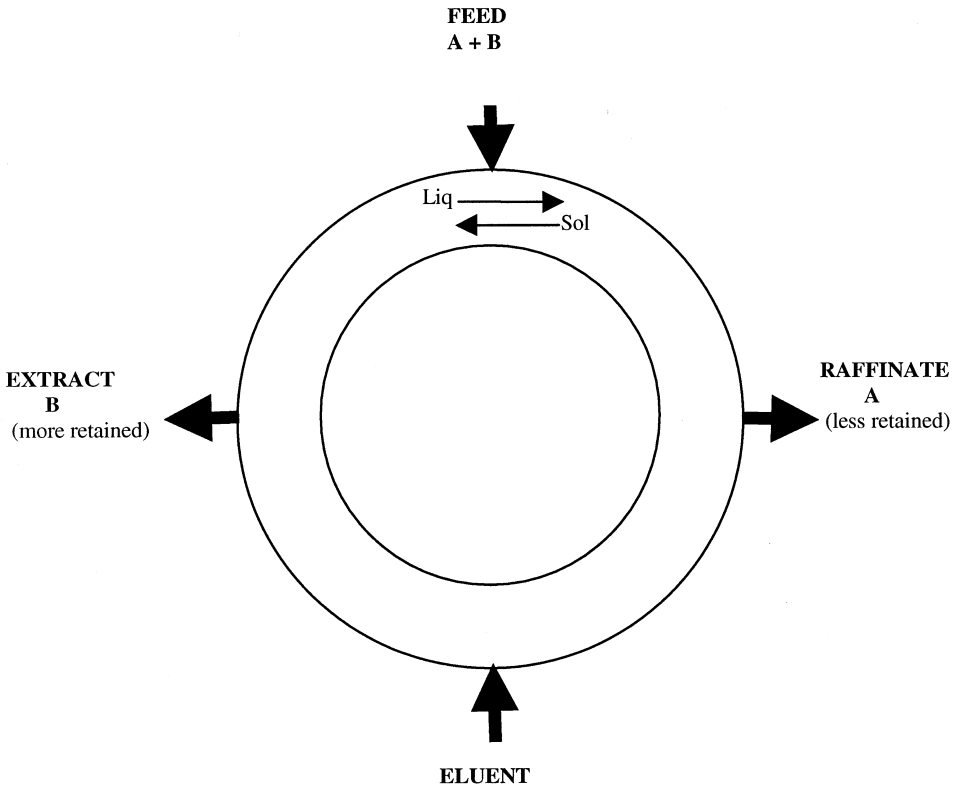

FIG. 1 The true moving bed.

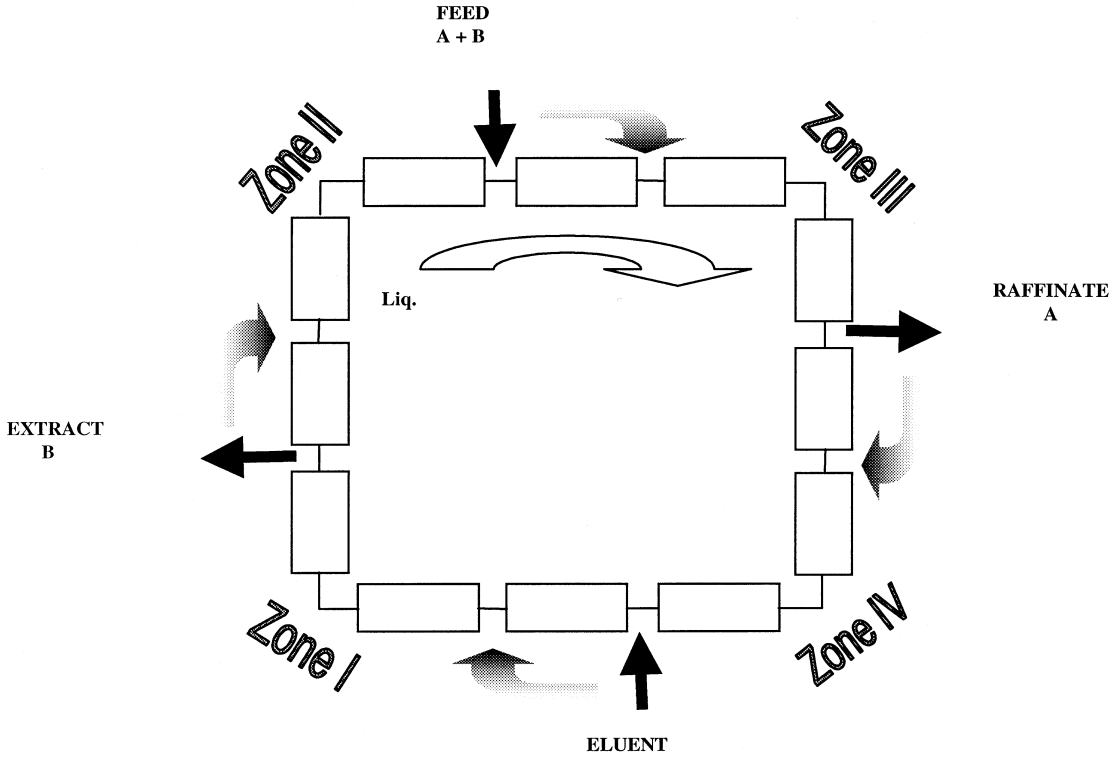

FIG. 2 The simulated moving bed.

MARCEL DEKKER, INC.
270 Madison Avenue, New York, New York 10016

nected, and the inlet and outlet positions are switched regularly to simulate the countercurrent movement of the sorbent. The TMB is then similar to a SMB with an infinite number of columns. However, it is possible to show that a configuration with a limited number of columns (8 to 12) is sufficient to obtain similar separation performances (10).

The internal flow rates of the SMB can be directly derived from the flow rates of the equivalent TMB (10).

In order to design an SMB, it is necessary to consider the finite number of theoretical plates of the columns. We estimate, by simulation, the number of columns per zone and the number of theoretical plates required in the system to reach the desired purity in the outlet lines with these calculated flow rates.

A limitation on the maximum pressure in the system and the number of theoretical plates required for separation must be determined before a system can be designed. For a given product separation, the column length and diameter can be optimized to give maximum productivity (11).

Pressure Drop

The pressure drop through the particle bed can be represented by different empirical correlations. For laminar flow through a monodispersed particle bed, an accurate pressure-drop correlation is obtained by the Kozeny–Karman equation (12):

$$\frac{\Delta P}{L} = h_k \mu a_p^2 \frac{(1-\varepsilon_e)^2}{\varepsilon_e^3} u = ku \tag{1}$$

where $\Delta P/L$ = pressure drop (Pa/m)
u = superficial velocity (m/s)
μ = viscosity (Pa·s)
ε_e = external porosity
a_p = specific area of particle (m^2/m^3)
h_k = coefficient $\cong$ 4.5 for spherical material

For the classical working conditions of HPLC separations, the laminar flow condition is

$$\mathrm{Re}_g = \frac{\rho u}{(1-\varepsilon_e) a_p \mu} \ll 1 \tag{2}$$

For spherical particles the specific area a_p is equal to $6/d_p$, where d_p is the particle diameter, Eq. (1) can then be expressed by

$$\frac{\Delta P}{L} = \frac{A}{d_p^2} u \tag{3}$$

MARCEL DEKKER, INC.
270 Madison Avenue, New York, New York 10016

where

$$A = 36 h_k \mu \frac{(1-\varepsilon_e)^2}{\varepsilon_e^3} \tag{4}$$

A is a function of the eluent properties but is independent of the particle size.

Consider an SMB configuration. The global pressure drop across the columns is obtained by summing the pressure drop over each column:

$$\frac{\Delta P}{L} = \frac{\sum_{i=1}^{N_{col}} \Delta P_i}{N_{col} L_{col}} = k\bar{u} \tag{5}$$

This relationship provides a definition of the mean fluid velocity $\bar{u}$ in the SMB system.

The SMB is a closed-loop system with a recycling pump. The highest pressure value in the system is therefore at the recycling pump outlet.

In order to work with a stable system, it is necessary to control the internal pressure of the system. One interesting way to do this is to regulate the suction pressure of the recycling pump by small variations of one of the inlet or outlet flow rates of the system. The classical method is to fix the suction pressure at a small value greater than zero to avoid cavitation in the recycling pump. This suction pressure is regulated by varying the extract flow rate. This allows us to work with stable inlet pressures in the system. If we consider that the pressure drops in the valves, connections, and tubing are negligible, the pressure at the recycling pump outlet is equal to the pressure drop across the columns plus the small pressure, set by regulation, at the recycling pump suction.

If P is the pressure limit in the system, the following limitation is required:

$$\Delta P + P_{rec.pump} \leq P_{max} \tag{6}$$

Finally, the pressure drop on the columns is limited by

$$\Delta P = kLu \leq \Delta P_{max} \tag{7}$$

Band Broadening in the Column

The number of theoretical plates of a chromatographic column N or the height equivalent to a theoretical plate $H = L_{col}/N$ is widely used to represent the band broadening in chromatographic columns (13).

Three independent factors are involved in the band-dispersion mechanism along a chromatographic column:

- Axial molecular diffusion. The molecules disperse or mix due to diffusion. Longitudinal diffusion (along the column axis) leads to band broadening of the chromatographic zone.

MARCEL DEKKER, INC.
270 Madison Avenue, New York, New York 10016

- Axial eddy diffusion. Band broadening is caused by different flow velocities through the column.
- Mass transfer resistance within the mobile and stationary phases.

These three effects can be well represented in the case of linear equilibrium with the classical Van Deemter (14) equation:

$$\begin{array}{ccccccc} H = & A & + & Bu & + & C/u & \\ & \text{Axial eddy diffusion} & + & \text{mass transfer resistance} & + & \text{axial molecular diffusion} & \end{array} \quad (8)$$

where u is the superficial mobile phase velocity.

In the working range of fluid velocity used in HPLC, the axial molecular diffusion is negligible and we can consider that

$$H = A + Bu \quad (9)$$

For a given stationary phase it is possible to estimate the values of the A and B parameters and to identify the influence of the particle size.

The origin, A, of the curve gives good information about the quality of the packing (14). This term represents the axial eddy dispersion and is proportional to the particle size. A value of 2 to 6 times the particle diameter is obtained with well-packed columns:

$$A = kd_p \quad (10)$$

The slope, B, of this curve represents the resistance to mass transfer. In the case of linear isotherms, this parameter can be expressed by (15)

$$B = \frac{2\dfrac{1-\varepsilon_e}{\varepsilon_e}\overline{K}}{\left(1+\dfrac{1-\varepsilon_e}{\varepsilon_e}\overline{K}\right)^2}\frac{t_m}{\varepsilon_e} \quad (11)$$

ε_e is the external porosity of the solid bed = 0.4, and t_m is the exchange time of the product in the particle. $\overline{K}$ is the retention factor of the product and can be determined from the retention time of an analytical injection by (16, 17)

$$\overline{K} = \frac{t_r - t_0}{t_0}\frac{\varepsilon_e}{1-\varepsilon_e} \quad (12)$$

where t_0 is the zero retention time of the column, expressed by

$$t_0 = \frac{\varepsilon_e V_{col}}{Q_{col}} \quad (13)$$

and t_r is the retention time of the product.

MARCEL DEKKER, INC.
270 Madison Avenue, New York, New York 10016

The exchange time can be estimated by knowing that kinetic limitations can be largely attributed to diffusional limitations occurring inside or outside the particles. The step associated with the adsorption itself is usually very fast and can be neglected. Convection in the pores can also be neglected. With these assumptions, the exchange time can be approximated to the diffusion time of the molecule in the particle: $t_m \cong t_d$. The total diffusion time is the sum of the external and internal diffusion of the molecule in the particle (18). The external diffusion obeys Fick's law through a motionless layer of fluid of thickness δ. The characteristic time for external diffusion can be then estimated:

$$t_e = \frac{V_p}{S_p}\frac{\delta}{D}\left(= \frac{d_p}{6}\frac{\delta}{D} \text{ for spherical particles}\right) \tag{14}$$

where D is the molecular diffusion coefficient of the molecule in the solvent. The thickness of the motionless layer can be estimated by Ranz and Levenspiel's correlation (18):

$$\mathrm{Sh} = d_p/\delta = 2 + 1.8\mathrm{Re}^{1/2}\mathrm{Sc}^{1/3} \tag{15}$$

The internal diffusion is approximated by the linear driving force (LDF) model (19, 20):

$$t_i = d_p^2/60\overline{D} \tag{16}$$

where $\overline{D}$ is the internal diffusion coefficient. As a rough approximation, one can guess that

$$\overline{D} \approx D/10 \tag{17}$$

The global diffusion time can then be estimated by (19)

$$t_d = t_e + \overline{K}t_i \tag{18}$$

where t_e and t_i are, respectively, the characteristic times for external and internal diffusion.

According to Eq. (11), the slope B is a function of the retention of the product [it increases with retention of the product (14)]. If the diffusion coefficients for both components are the same, the number of theoretical plates for a given fluid velocity will then be smaller for the more retained component. If the simulation shows that N_{min} theoretical plates are required for the desired separation performance, we must choose the working conditions by considering the limitation by the more retained component B in zone I of the SMB, where the highest fluid velocity u_I occurs, leading to

$$N_B = \frac{L}{H_B} = \frac{L}{A_B + B_B u_I} \geq N_{min} \tag{19}$$

where L is the sum of the column lengths of the SMB. This calculation is only valid for linear adsorption isotherms. In the case of nonlinear adsorption isotherms, the band broadening can be well estimated by this method by using the initial slope of the adsorption isotherm $\overline{K}_i$ to calculate the influence of the resistance to the mass transfer (10).

SMB Working Conditions

The required number of theoretical plates (19) and the pressure drop limit (7) of the system must be taken into account in the SMB design, leading to the following set of inequalities:

$$\left.\begin{aligned} N_B = \frac{L}{H_B} = \frac{L}{A_B + B_B u_I} \geq N_{min} \\ \Delta P = kL\bar{u} \leq \Delta P_{max} \end{aligned}\right\} \tag{20}$$

The objective in designing an industrial process is usually to minimize the separation cost. The cost of investment is influenced by two parameters:

- The cost of the SMB hardware.
- The cost of the stationary phase.

Depending on the cost ratio of the system and of the stationary phase, it is possible to use the following definitions of the productivity to characterize the performance of the system (11): The *productivity per column cross section unit* of the system is defined as

$$\Phi_S = \frac{Q_{feed} C_{feed}}{\Omega} \text{ (kg racemate/m}^2\text{/day)} \tag{21}$$

The productivity Φ_S is related to the column cross section. This definition is useful if the column diameter is a key factor of the separation cost. This is true if the hardware represents the major part of the investment.

The *productivity per column volume unit* of the system is defined as

$$\Phi_V = \frac{Q_{feed} C_{feed}}{V_{CSP}} \text{ (kg racemate/m}^3\text{/day)} \tag{22}$$

The productivity Φ_V is related to the volume of the stationary phase in the SMB columns. This definition should be used if the required stationary phase is expensive and represents an important fraction of the separation cost.

This definition is therefore useful for chiral applications: the chiral packing material is usually expensive and often represents a significant part of the investment (21). This cost is not a function of the particle size for chiral packings such as derivatized polysaccharide-coated silica, the most popular type

used for chromatographic enantioseparations. Therefore, the required amount of stationary phase must be optimized.

The optimal working conditions are then obtained (11) when

$$\left.\begin{aligned} N_{\mathrm{B}} = \frac{L}{H_{\mathrm{B}}} = \frac{L}{A_{\mathrm{B}} + B_{\mathrm{B}} \dfrac{Q_{\mathrm{I}}}{\Omega}} = N_{\min} \\ \Delta P = kL \frac{\overline{Q}}{\Omega} = \Delta P_{\max} \end{aligned}\right\} \tag{23}$$

where Ω is the column section and $\overline{Q} = \Omega\overline{u}$ is the mean flow rate in the SMB.

EXPERIMENTAL

A chiral stationary phase available at two different particle sizes (20 and 50 μm) was experimentally studied to estimate the separation performances of an SMB process and the cost of the separation when using the two particle sizes. Analytical HPLC system:

- Spectra-physics Isochrom SP 8810-020 LC pump.
- KNAUER Variable wavelength Monitor type 87.00.
- Spectra-Physics DataJet-Integrator.
- Sample injection system: Rheodyne 7125.
- Column thermostat Jetstream 2.

Stationary phase: Chiralcel OD 20 μm, Chiralcel OD 50 μm (ChiralTech, Illkirch) slurry-packed into 250 4.6 mm I.D. stainless steel columns.
Mobile phase: *n*-Heptane and isopropanol were of Merck Lichrosolv quality.
Sample: Methyl mandelate, Sigma-Aldrich.

Separation Conditions

The separation of the racemic mixture of methyl mandelate was performed at 30°C with a mixture of *n*-heptane/2-propanol 90/10 (v/v) as eluent on the two analytical columns packed with the two samples of Chiralcel OD.

EXPERIMENTAL RESULTS

Particle Size of the Stationary Phases

The mean particle size was accurately measured by laser diffraction. The mean particle size thus determined was found to be slightly different from the claimed values: 25 μm instead of 20 μm and 51 μm instead of 50 μm. The distribution of particle sizes was very small for both samples.

TABLE 1
Retention of Methyl Mandelate Enantiomers on Chiralcel OD 25 and 51 μm

Stationary phase	tr_1 (min)	tr_2 (min)	$\overline{K}_1$	$\overline{K}_2$	Selectivity, $\alpha = \overline{K}_2/\overline{K}_1$
Chiralcel OD, 25 μm	7.1	10.6	2.18	3.58	1.64
Chiralcel OD, 51 μm	7.2	11	2.22	3.74	1.68

Adsorption Isotherms

Consider a stationary phase available at different particle sizes. In most cases the assumption that the phase has the same properties is verified (22): the specific pore volume, the concentration sites, the specific interfacial area, and the selector molecule is assumed to be similar, leading to adsorption isotherms independent of the particle size. The retention factor can be determined from the retention time of an analytical injection by Eq. (12).

The analytical injection of methyl mandelate into the two columns leads to a variation of less than 5% on the retention times for both compounds (Table 1). Furthermore, the selectivity is similar (Fig. 3).

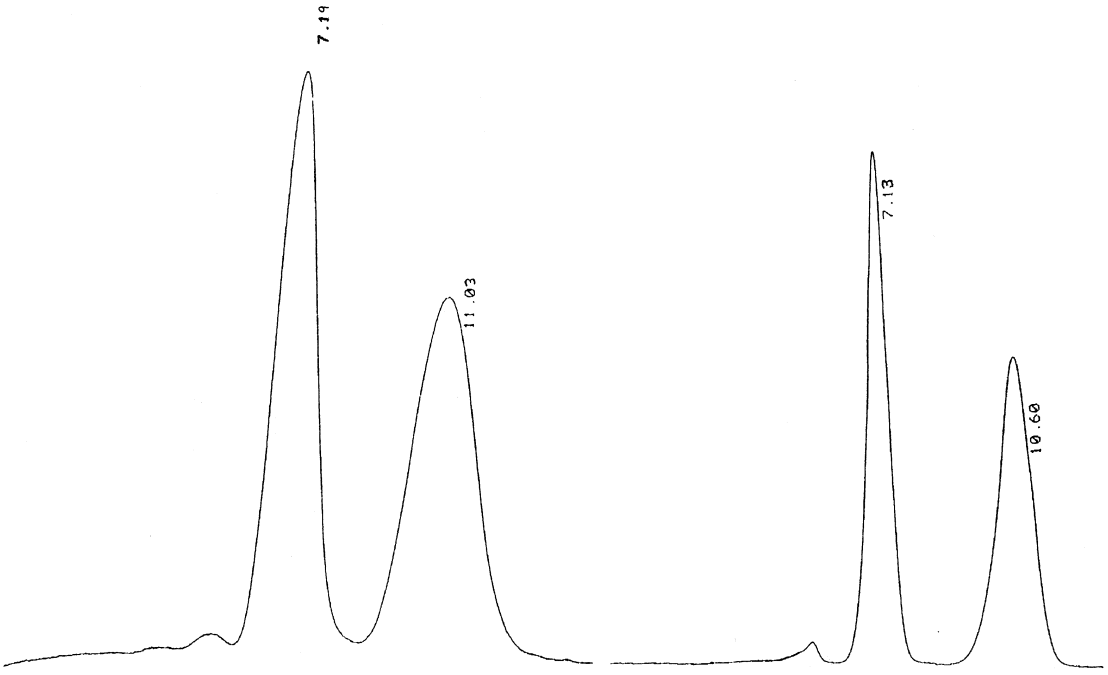

FIG. 3 Analytical injection of methyl mandelate on Chiralcel OD 25 μm (right peaks) and 51 μm (left peaks). Analytical column (4.6/250 mm), temperature 30°C, flow rate = 1 mL/min. Injection of 10 μL at 1 g/L. Eluent: *n*-Heptane/2-propanol (90/10 v/v). UV detection λ = 254 nm.

MARCEL DEKKER, INC.
270 Madison Avenue, New York, New York 10016

If we consider the adsorption isotherms to be similar, the particle size will only modify the hydrodynamic behavior of the columns. Only the pressure drop and the hydrodynamic dispersion will be influenced by variation of the particle size.

Pressure Drop

The pressure drop can be estimated theoretically according to the Kozeny–Karman Eq. (1). The stationary phase particles are monodispersed and spherical. The viscosity of the eluent is about 0.55 cP. The external porosity of the packed column can be considered to be 0.4 for well-packed columns.

According to Eq. (3), the theoretical pressure drop is given by

$$\frac{\Delta P}{L} = \frac{0.501}{d_p^2} u \tag{24}$$

The pressure drop has been measured on the analytical columns. As shown by Fig. 4, the theoretical law follows the experimental points with very good accuracy.

Band Dispersion in the Column

The theoretical value of the height equivalent to a theoretical plate can be calculated, using Eqs. (9) to (18). The following data have been used for this calculation:

- Solvent viscosity: 0.55 cP.
- Solvent density: 0.7.
- Molecular diffusion coefficient of methyl mandelate in the eluent.

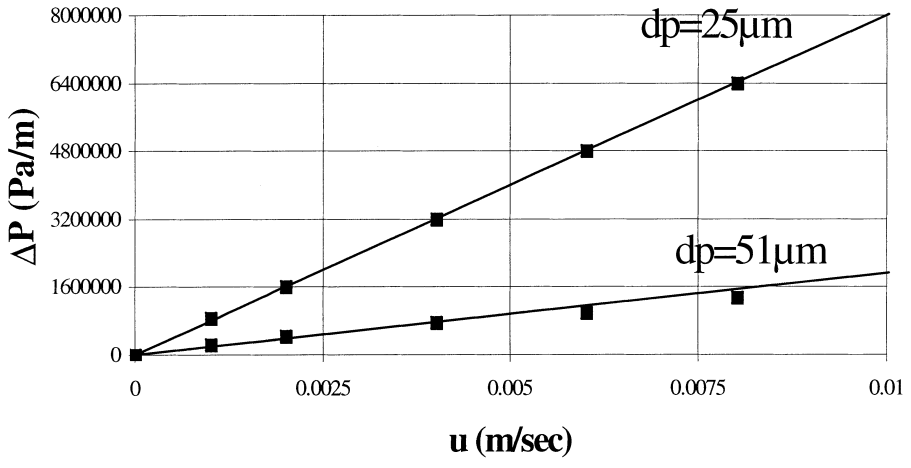

FIG. 4 Influence of the fluid velocity on the pressure drop. Pressure drop on analytical columns (4.6/250 mm) packed with Chiralcel OD 25 µm and 51 µm. Eluent: *n*-Heptane/2-propanol (95/5 v/v). Temperature 30°C. Points: Experimental measurements. Lines: Theoretical value.

MARCEL DEKKER, INC.
270 Madison Avenue, New York, New York 10016

The Wilke–Chang equation (23) can be used to predict the diffusion coefficient of solute M at very low concentration in solvent S:

$$D = 8.7 \times 10^{-15} \frac{(\Phi M_S)^{1/2} T}{\eta_S V_M^{0.6}} \tag{25}$$

where D = diffusion coefficient (m^2/s)
ϕ = association factor of solvent S. $\phi = 1.0$ for unassociated solvent
M_S = molecular weight of the solvent. The eluent is a binary mixture

We can consider a mean value of $M_s = 99$ g/mol
T (temperature) = 298 K
η_s (solvent viscosity) = 0.55×10^{-3} Pa·s
V_M (molar volume of solute M at normal boiling temperature) ≅ 178 cm^3/mol (24)

We then get

$$D \cong 2.1 \times 10^{-9}\ m^2/s$$

and internal diffusion coefficient

$$\overline{D} \cong D/10 \cong 2.1 \times 10^{-10}\ m^2/s$$

According to these values, it is possible to calculate the internal and external diffusion times using Eqs. (14) and (16). The influence of both internal and external diffusion on the global diffusion time is estimated according to Eq. (18) for different fluid velocities and different particle sizes. In this case it is possible to show that the external diffusion is negligible compared to the internal diffusion. Even for small particle sizes and small fluid velocities the external diffusion term is still negligible compared with the internal diffusion (with $d_p = 2$ μm and $u = 5 \times 10^{-4}$ m/s, more than 90% of the global diffusion is still due to the interparticle mass transfer resistance).

The number of plates in each column has been experimentally evaluated at different fluid velocities using the tangential measurement of the base peak width: $N = 16(t_r/w)^2$ (25). The experimental points presented in Fig. 5 can be compared with the theoretical value obtained from Eqs. (9) to (18) represented by continuous lines. The column efficiency estimated by the theoretical approach is in good agreement with the practical results. The resistance to mass transfer in the separation example is mainly due to internal diffusion. Slope B of Eq. (9) is therefore proportional to the internal diffusion $\overline{D}$ coefficient according to Eqs. (11), (16), and (18). The estimation of $\overline{D}$ by Eq. (17) is therefore an accurate description of the coated silica stationary phase.

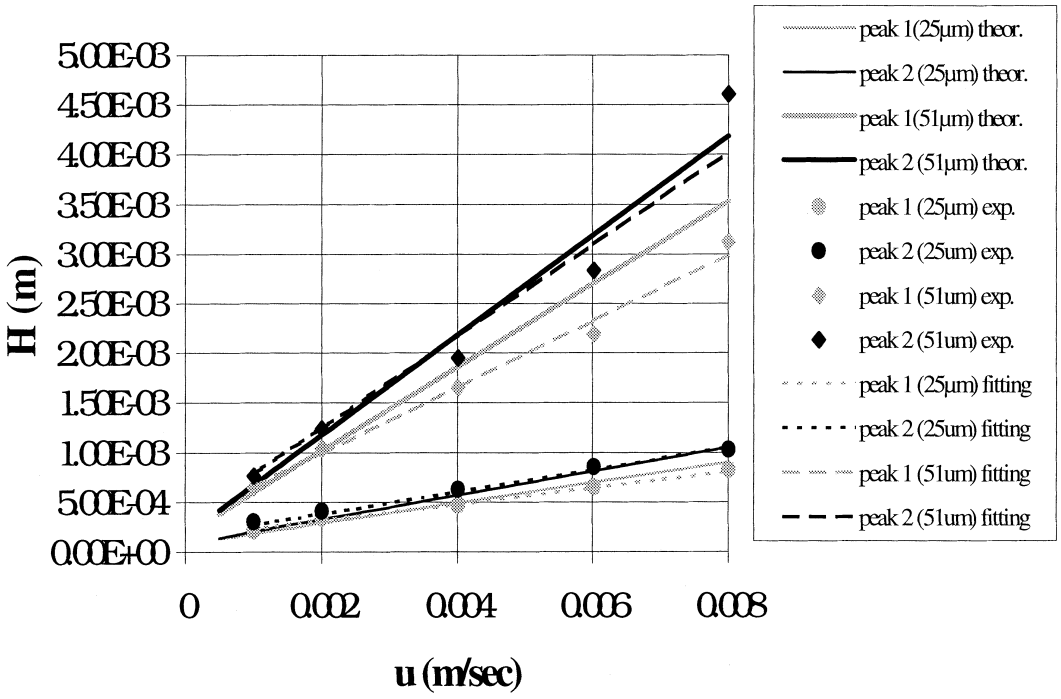

FIG. 5 Influence of the fluid velocity on the height equivalent to a theoretical plate. Measured on analytical columns (4.6/250 mm) packed with Chiralcel OD 25 µm and 51 µm. Injection of a racemic mixture of methyl mandelate. Eluent: *n*-Heptane/2-propanol (95/5 v/v). Temperature 30°C. Points: Experimental values. Continuous lines: Theoretical model. Dashed lines: Fitted curves.

Because the external diffusion is negligible compared to the internal diffusion, it is possible to show the influence of the particle size on Eq. (9) (15):

$$H = A' d_p + B' d_p^2 u \tag{26}$$

The experimental results have been fitted (dashed lines on Fig. 5) by using Eq. (26), leading to

$$H_A = 6d_p + 1.28 \times 10^8 \, d_p^2 u \qquad \text{for the less retained product} \tag{27}$$

$$H_B = 6d_p + 1.78 \times 10^8 \, d_p^2 u \qquad \text{for the more retained product} \tag{28}$$

These fitted equations will be used to estimate the influence of particle size on SMB performance.

ESTIMATION OF THE SMB PERFORMANCE

Consider linear adsorption isotherms (this assumption is only true for small feed concentrations). The TMB flow rates can be calculated for this separation (3) with a reflux ratio γ.

MARCEL DEKKER, INC.
270 Madison Avenue, New York, New York 10016

$$\left.\begin{aligned} Q_{\mathrm{I}_{\mathrm{TMB}}} &= \gamma \overline{K}_2 \dot{M} \\ Q_{\mathrm{II}_{\mathrm{TMB}}} &= \gamma K_1 \dot{M} \\ Q_{\mathrm{III}_{\mathrm{TMB}}} &= (K_2/\gamma)\dot{M} \\ Q_{\mathrm{IV}_{\mathrm{TMB}}} &= (\overline{K}_1/\gamma)\dot{M} \end{aligned}\right\} \tag{29}$$

A reflux ratio of 1 corresponds to the highest possible productivity using an ideal TMB system without dispersion in the columns (infinite number of plates) to reach 100% purity for both extract and raffinate. For a real system the reflux ratio is increased to take into account the limitation due to the dispersion and also to improve the robustness of the process (10). The target purity is fixed at 99% for extract and raffinate. For this high a purity we fix the reflux ratio at $\gamma = 1.04$, corresponding to a robust system that requires an acceptable number of plates.

The SMB internal flow rates and the shift period can be calculated (3) by

$$Q_{i_{\mathrm{SMB}}} = Q_{i_{\mathrm{TMB}}} + \frac{\varepsilon}{1-\varepsilon}\dot{M} \qquad i = \mathrm{I\ to\ IV} \tag{30}$$

$$\Delta T = \frac{1-\varepsilon}{\dot{M}} V_{\mathrm{col}} \tag{31}$$

The feed flow rate is directly calculated by the difference of the flow rates in zones III and II and can therefore be directly expressed by

$$Q_{\mathrm{f}} = Q_{\mathrm{III}_{\mathrm{SMB}}} - Q_{\mathrm{II}_{\mathrm{SMB}}} = \left(\frac{\overline{K}_2}{\gamma} - \gamma K_1\right)\dot{M} \tag{32}$$

The retention factors $\overline{K}_1$ and $\overline{K}_2$ have been estimated experimentally (Table 1). With a reflux ratio of $\gamma = 1.04$, the SMB flow rates and the shift period can then be calculated (3).

$$\left.\begin{aligned} Q_{\mathrm{I}_{\mathrm{SMB}}} &= 3.757 Q_{\mathrm{f}} \\ Q_{\mathrm{II}_{\mathrm{SMB}}} &= 2.517 Q_{\mathrm{f}} \\ Q_{\mathrm{III}_{\mathrm{SMB}}} &= 3.517 Q_{\mathrm{f}} \\ Q_{\mathrm{IV}_{\mathrm{SMB}}} &= 2.370 Q_{\mathrm{f}} \\ \Delta T &= 0.704 V_{\mathrm{Col}}/Q_{\mathrm{f}} \end{aligned}\right\} \tag{33}$$

These parameters are related to the feed flow rate and to the column volume V_{col}. These parameters will be optimized to reach the optimal productivity of the SMB system by using the set of Eq. (23). Therefore,

the pressure drop and the hydrodynamic dispersion of the columns will be studied.

The SMB process has been simulated to estimate the required number of plates to reach a purity of extract and raffinate higher than 99% by using two columns per SMB zone with this set of flow rates. The classical equilibrium stage model will be used for this calculation: The columns of the SMB process are considered to be an association of mixing cells in series, where the adsorption equilibrium is assumed to be reached in each cell.

The following mass balance can be written for component i in cell k for each column of the SMB:

$$C_i^{k+1} = C_i^k + \frac{\dfrac{\varepsilon V_{\text{col}}}{Q_{\text{col}}}\left(1 + \dfrac{1-\varepsilon}{\varepsilon}\overline{K}_i\right)}{J}\frac{dC_i^k}{dt} \tag{34}$$

where J is the theoretical number of cells of the column
$\varepsilon V_{\text{col}}/Q_{\text{col}}$ is the zero retention time of the column

The proper boundary conditions have to be used to correctly simulate the SMB process. It is then possible to search for the number of theoretical plates required to reach the given purities for the extract and raffinate streams. According to the simulation, a purity of 99% of both extract and raffinate can be obtained with 300 plates in the system with this set of flow rates (33). The steady-state internal concentration profile calculated at half-period is presented in Fig. 6.

The maximum pressure drop was fixed at 60 bars for the system.

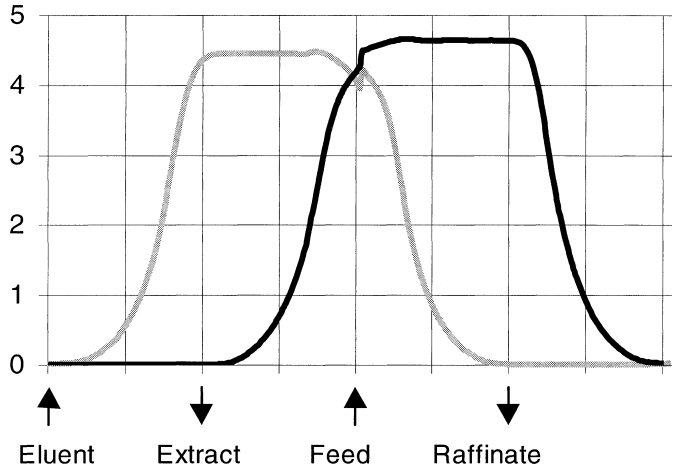

FIG. 6 Simulation of the SMB. Internal concentration profile with 300 plates.

The optimal hydrodynamic working conditions are obtained if the set of Eq. (23) is verified, using the experimental measurements

$$\left.\begin{array}{c} \dfrac{L}{6d_{\mathrm{p}} + 1.78 \times 10^{8}\, d_{\mathrm{p}}^{2}\, \dfrac{Q_{\mathrm{I}}}{\Omega}} = 300 \\ \\ \dfrac{0.501}{d_{\mathrm{p}}^{2}} L\, \dfrac{\overline{Q}}{\Omega} = 60 \times 10^{5} \end{array}\right\} \tag{35}$$

According to Eq. (33), we have $Q_{\mathrm{I}} = 3.757 Q_{\mathrm{f}}$ and $\overline{Q} = 3.040 Q_{\mathrm{f}}$. Therefore:

$$\left.\begin{array}{c} \dfrac{L}{6d_{\mathrm{p}} + 6.69 \times 10^{8}\, d_{\mathrm{p}}^{2}\, \dfrac{Q_{\mathrm{f}}}{\Omega}} = 300 \\ \\ \dfrac{1.523}{d_{\mathrm{p}}^{2}}\, L\, \dfrac{Q_{\mathrm{f}}}{\Omega} = 60 \times 10^{5}\} \end{array}\right\} \tag{36}$$

In order to study the influence of particle size on performance, the two following equations can be obtained by substitution:

$$L = 8L_{\mathrm{col}} = \frac{2.408 \times 10^{18}\, d_{\mathrm{p}}^{3}}{\sqrt{7.515 \times 10^{6} + 7.336 \times 10^{18}\, d_{\mathrm{p}}^{2}} - 2741.4} \tag{37}$$

$$\frac{Q_{\mathrm{f}}}{\Omega} = \frac{\sqrt{7.515 \times 10^{6} + 7.336 \times 10^{18}\, d_{\mathrm{p}}^{2}} - 2741.4}{6.113 \times 10^{11}\, d\mathrm{p}} \tag{38}$$

According to Eqs. (37) and (38), the column length and the ratio Q_{f}/Ω required to perform at optimal productivity are direct functions of the particle diameter.

The ratio Q_{f}/Ω can be used to solve two kinds of problems:

- For a given required production, the SMB design can be used to estimate the optimal column section Ω needed to work with the required feed flow rate Q_{f}.
- For a given SMB system where the column section Ω is fixed, the feed flow rate can be calculated, allowing the optimum production rate of the process to be predicted.

Consider the first case: the SMB will be designed to separate 10 metric tons of methyl mandelate per year. The feed concentration is equal to 10 g/L, assuming linear adsorption isotherms for the two enantiomers. Assuming 8000 working hours a year, the corresponding feed flow rate is 125 L/h.

The influence of the particle size on the column length and diameter can be calculated according to Eqs. (37) and (38). Figure 7 represents the influence of the particle size on the column size. For particles smaller than 20 μm, the required column length is smaller than 5 cm. However, good packing quality using small particles cannot be easily achieved for preparative columns with large diameters if the packed bed is too short. A minimum bed length of 5 cm is therefore required. *The minimum required particle size is therefore about* 20 μ*m for this separation to work with an acceptable column length (>5 cm*).

For particles larger than 20 μm, the required column diameter is about 11 cm, whatever the particle size, for the production of 10 metric tons per year. The column diameter required decreases with increasing particle size, but this variation is only significant for very small particle sizes (<15 μm). For $d_p >$ 15 μm, the axial Eddy diffusion term (proportional to d_p) in Eq. (9) becomes negligible compared to the mass transfer resistance term (proportional to d_p^2). In this case the solution of the set of Eq. (36) can be simplified and the influence of d_p in Eq. (38) disappears. The required column diameter is therefore independent of the particle size.

In conclusion, for particle sizes larger than 15 μm, the required column diameter is almost independent of particle size.

On the other hand, the required column length increases drastically with particle size. If the particle size is increased from 25 to 51 μm, the required optimal column length is increased from 7.2 to 29.5 cm for the same production of 10 metric tons per year.

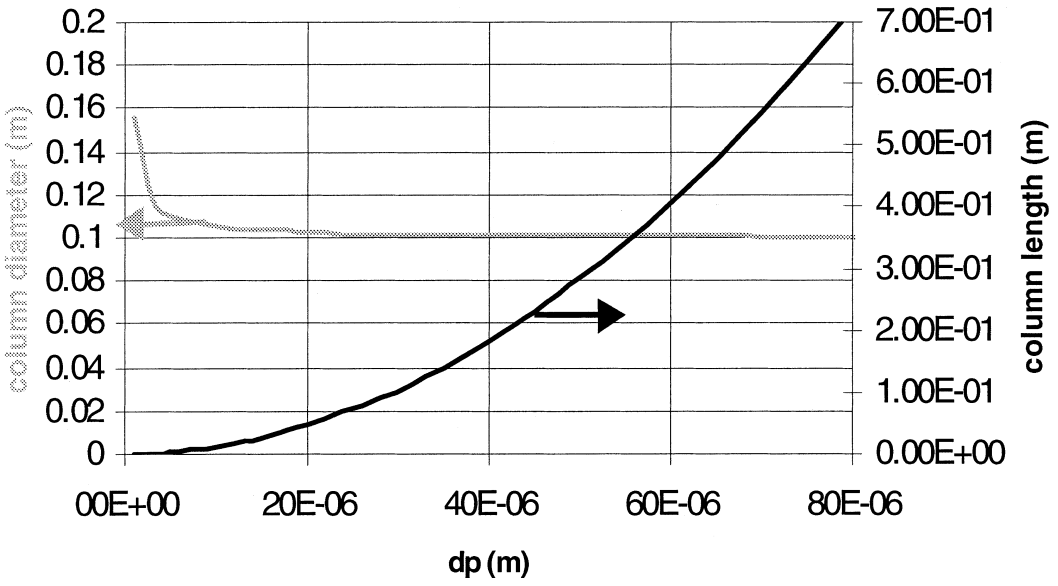

FIG. 7 Influence of the particle size on the column size.

In conclusion, increasing the particle size tends to increase the required optimal length of the columns. The required amount of stationary phase is therefore increased by increasing the particle size, and the investment for packing is thus about four times higher using Chiralcel OD 51 μm than 25 μm packing.

Particle size therefore has a significant effect on the productivity of the system, as defined by Eqs. (21) and (22) (Fig. 8): 20 μm is the smallest particle size one can use to work with an acceptable column length.

When the particle size is larger than 20 μm, it can be seen from Fig. 8 that the productivity per column cross section unit Φ_S slowly increases with increasing particle size. This effect is due to the evolution of the required column diameter shown in Fig. 7. However, the influence of the particle size is very small and only significant for very small particles. Productivity is approximately independent of particle sizes over 20 μm. *The productivity per column cross-section unit Φ_S of the SMB process (using the same column diameter) is therefore almost the same whether using Chiralcel OD 25 or 51 μm (Φ_S is increased by 2% with the 50 μm material).*

The influence of particle size is, however, much more important on the productivity per column volume unit Φ_V. *The required column length is drastically increased by increasing the particle size, leading to a significant increase in the amount of stationary phase required in the column.*

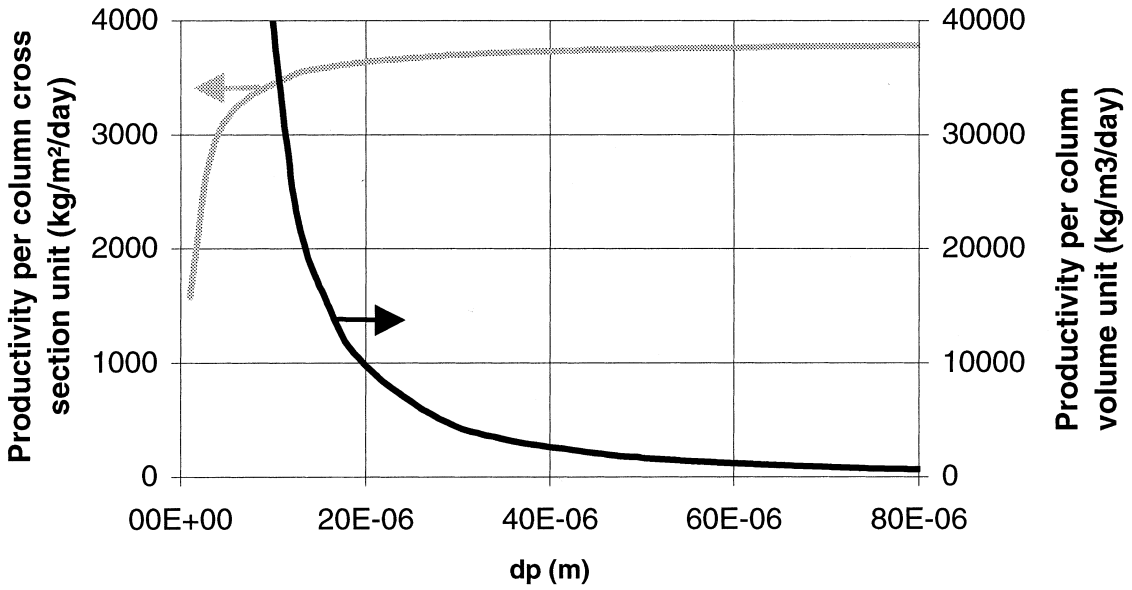

FIG. 8 Influence of the particle size on the SMB productivity.

MARCEL DEKKER, INC.
270 Madison Avenue, New York, New York 10016

The smallest particle size* therefore leads to the highest productivity per column volume unit, corresponding to the smallest required column length. When using an expensive chiral stationary phase, it is very important to minimize the required amount of stationary phase. As the productivity per column cross-section unit Φ_S is almost the same for $d_p > 20$ μm, the productivity per column volume unit allows one to predict the evolution of the separation cost of the process.

If the column diameter is fixed, using Chiralcel OD 51 μm instead of 25 μm leads to almost the same production per time unit, but the required amount of stationary phase is drastically increased for the same production capacity. *For a given production capacity, the investment in packing is therefore about four times higher with Chiralcel OD 51 μm than with 25 μm packing.*

CONCLUSION

Particle size is a key factor for the optimization of chiral SMB separations, where the packing cost often represents a significant part of the investment. In the case of linear adsorption isotherms and for products having almost the same diffusion coefficients, it is possible to show that particles sizes of 20–25 μm lead to optimum separation performance: the productivity related to the required amount of stationary phase is then maximized. This conclusion could also be verified in the case of nonlinear isotherms.

NOTATION

a_p	specific area of particles
A, B, C	coefficients relating the height equivalent to a theoretical plate to the mobile phase velocity
C_{feed}	feed concentration
D	molecular diffusion coefficient
$\overline{D}$	internal diffusion coefficient
d_p	particle size
h_k	Kozeny coefficient
H	height equivalent to a theoretical plate
k	parameter relating the pressure drop to the mobile phase velocity

* For very small particle size, the influence of axial molecular diffusion in Eq. (8) tends to increase. This term is neglected in our calculation. However, it is easy to show that even with a particle size of $d_p = 1$ μm, axial molecular diffusion represents less than 1.6% of the total dispersion at the corresponding operating conditions of the SMB system (mean fluid velocity of 0.0055 m/s).

MARCEL DEKKER, INC.
270 Madison Avenue, New York, New York 10016

$\overline{K}_i$	initial slope of the adsorption isotherm
L_{col}	column length
L	sum of the column lengths of the SMB
$\dot{M}$	solid flow rate
N_i	number of columns in zone i
N	number of theoretical plates
N_{min}	minimum number of plates required
P_{max}	maximum pressure acceptable
$P_{rec.pump}$	suction pressure of the SMB recycling pump
Q_{col}	flow rate in the column
$Q_{k_{TMB}}$, $Q_{k_{SMB}}$	TMB and SMB internal flow rates in zone k
Q_{feed}	feed flow rate
$\overline{Q}$	mean internal flow rate SMB
t_0	zero retention time
tr_i	retention time component i
t_d	global diffusion time in the particle
t_e	external diffusion time in the particle
t_i	internal diffusion time in the particle
t_m	exchange time of the molecule in the particle
u	mobile phase velocity
$\overline{u}$	SMB average mobile phase velocity
V_{col}	SMB column volume
V_{CSP}	volume of chiral stationary phase in the SMB
ΔP	pressure drop
ΔP_{max}	maximal pressure drop on the SMB column
ΔT	period
δ	thickness of the motionless layer of fluid around the particle
ε_e	external porosity
ρ	solvent density
μ	mobile phase viscosity
Ω	column section
γ	margin factor on the TMB flow rates
	separation selectivity
Φ_S	SMB productivity per column cross section unit ($kg/m^2 \cdot$column/day)
Φ_V	SMB productivity per column volume unit ($kg/m^3 \cdot$column/day)
Re_g	particle Reynolds number
Re	Reynolds number
Sc	Schmidt number
Sh	Sherwood number

REFERENCES

1. D. B. Broughton, US Patent 2,985,589 (1961).
2. P. Deckert and W. Arlt, *Chem.-Ing.-Tech.*, *66*(10), 1334–1340 (1994).
3. R. M. Nicoud, *LC-GC Intl.*, *5*, 43 (1992).
4. E. Francotte, *J. Chromatogr. A*, *666*, 565 (1994).
5. S. Allemark and V. Schurig, *J. Mater. Chem.*, *7*(10), 1955–1963 (1997).
6. M. N. Cayen, *Chirality*, 1991, *3*, 94–98 (1991).
7. D. M. Ruthven and C. B. Ching, *Chem. Eng. Sci.*, *44*, 1011–1038 (1989).
8. G. Storti, R. Baciocchi, M. Mazzotti, and M. Morbidelli, *Ind. Eng. Chem. Res.*, *34*, 288–301 (1995).
9. M. Mazzotti, G. Storti, and M. Morbidelli, *J. Chromatogr. A*, *769*, 3–24 (1997).
10. D. Tondeur and M. Bailly, in *Simulated Moving Bed*: *Basics and Applications*, R. M. Nicoud, Ed., INPL, Nancy, France, 1993, pp. 95–117.
11. F. Charton and R. M. Nicoud, *J. Chromatogr. A*, *702*, 97–112 (1995).
12. J. S. B. Kozeny, *Akad. Wiss. Wien Abt. IIa*, *136*, 271 (1927).
13. A. J. P. Martin and R. L. M. Synge, *Biochem. J.*, *35*, 1359 (1941).
14. J. J. Van Deemter, F. J. Zuiderweg, and A. Klinkenberg, *Chem. Eng. Sci.*, *5*, 271–289 (1956).
15. J. Villermaux, *Ser. Espec*: *Appl. Sci.*, *33*, 83–140 (1981).
16. B. L. Karger, L. R. Snyder, and C. Horvath, *Introduction to Separation Science*, Wiley, New York, NY, 1973.
17. L. R. Snyder and J. J. Kirkland, *Introduction to Modern Liquid Chromatography*, Wiley, New York, NY, 1979.
18. J. Villermaux, *Génie de la réaction chimique*, *conception et fonctionnement des réacteurs*, 2nd ed., TEC & DOC—Lavoisier Publisher, 1993.
19. J. Villermaux, *J. Chromatogr. 409*, 11 (1987).
20. D. R. Ruthven and C. B. Ching; *Preparative and Production Scale Chromatography* (edited by G. Ganestos and P. E. Barker, Chromatographic Science Series), Dekker, New York, NY, 1993.
21. R. M. Nicoud, *Proceedings of the Chiral Europe 96*, *Stasburg*, *14–15 October 1996*, Spring Innovations Ltd Publisher, SK7 1BA, 1996.
22. A. Felinger and G. Guiochon, *J. Chromatogr.*, *591*, 31 (1992).
23. C. R. Wilke and P. Chang, *Am. Inst. Chem. Eng. J.*, *1*, 264 (1955).
24. *Perry's Chemical Engineer's Handbook*, 6th ed., McGraw-Hill, New York, NY.
25. R. Rosset, M. Caude, and A. Jardy, *Chromatographies en phase liquide et supercritique*, Masson Publisher, 1991.

Received by editor February 16, 1999
Revision received December 1999

Request Permission or Order Reprints Instantly!